Probing viscoelastic properties of a thin polymer film sheared between a beads layer and an ultrasonic resonator

J. Léopoldès[(a)] and X. Jia[(b)]

Laboratoire de Physique des Matériaux divisés et Interfaces, Université Paris Est, CNRS UMR 8108
Cité Descartes, 77454 Marne-la-Vallée cedex 2, France, EU

Abstract – We report a study of viscoelastic properties of thin polymer films of $10-250$ nm at the MHz range. These thin films are confined between a quartz crystal resonator and a millimetric bead layer, producing an increase of both resonance frequency and dissipation of the quartz resonator. For the elastic film, both shear modulus and dynamic viscosity are extracted from these ultrasonic measurements. For the liquid film, the ageing effects are observed on both elastic and dissipative responses and the loss angle of the film is determined. This modified quartz resonator thus provides an effective tool for probing the rheological properties of viscoelastic thin films at ambient environment.

Introduction. – Viscoelastic layers confined into small volumes are ubiquitous in nature and are known to alter friction and adhesion at a solid-solid interface [1–4]. However, conventional mechanical testing is not adapted for thin-film investigation and specific metrology is needed. Naturally occurring instabilities such as wrinkling or dewetting provides valuable information about rheological and mechanical properties of thin polymer films [5,6]. Oscillatory interfacial rheology conducted with a tribometer [7], the Surface Force Apparatus [8,9] and Atomic Force Microscopy [10], offers a complementary description of thin films over several decades of frequency. Note that the rheological behavior at high frequency cannot be investigated with these techniques, yet it is important for applications such as hard-disk drives. Moreover, for polymers the time-temperature superposition principle cannot always be used to obtain the high-frequency response because crystallization may arise at low temperature.

Acoustic-wave devices have proven to be suitable for the high-frequency investigation [11,12] of thin films of thicknesses ranging from nanometers up to microns length scales. For example, the mechanical properties of the nanometric films can be measured using ultrasound resonant spectroscopy via its resonant modes, excited directly by the ultrafast pulsed-laser irradiation [13]. Alternatively the film properties can be extracted from the interaction with an acoustic sensor. Among others, quartz crystal (AT-cut) resonators operating in shear mode at ultrasonic frequency from 1–100 MHz have been the most widely used to monitor the viscoelastic properties of thick films of thickness $h > 1\,\mu$m adsorbed on their surfaces [11]. In this case the interaction between the resonator and the film modifies the resonance of the quartz and the resulting frequency shift provides some information about the film. However for thin films, *i.e.* $h < 1\,\mu$m, no significant shear strain is produced inside it because the film is located at an antinode of the standing wave. In such a case, the shift of resonance frequency is only a function of the mass alone and the acoustic properties of the film may be ignored (quartz crystal microbalance QCM). Nevertheless, for mechanical probing it is still possible to use composite resonators. For example, coating the film of interest with a second overlayer (sandwich configuration) allows enhancing the shear stress and characterizing its rheological properties down to nanometric thicknesses [14].

In this letter, we describe another approach to probe the viscoelastic properties of thin polymer films, elastic (crosslinked) and liquid, by using a conventional QCM. To this end, we deposit gently a layer of spherical beads on the top of a film of thickness $h \sim 10$–250 nm coated on

[(a)]E-mail: julien.leopoldes@univ-mlv.fr
[(b)]E-mail: jia@univ-mlv.fr
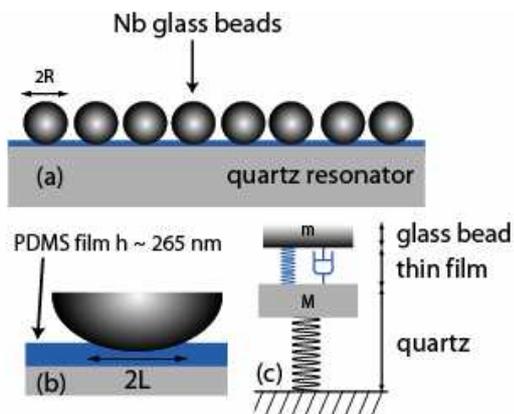
Fig. 1: (Colour on-line) (a) Sketch of the experiment, (b) coupling between a sphere and the quartz and (c) a viscoelastic model of the coupled oscillators.

the surface of the ultrasonic resonator. The relative motion (out-of-phase) between the quartz and the beads through the film will modify the resonance response of the quartz crystal. We show how the resulting shifts of frequency Δf and inverse quality factor ΔQ^{-1} can be related directly to the elastic and viscous moduli of a crosslinked film.

Experimental setup. – We study polydimethylsiloxane (PDMS) films of crosslinked Sylgard 184 and of liquid polymer ($M_w \sim 90000$, 170000) deposited on a quartz resonator of $f_0(= \omega_0/2\pi) \sim 5$ MHz (Maxtek) (fig. 1(a)). The surface of the crystal is polished and gold-coated with a roughness of about $\sigma \sim 2$ nm. This quartz is cleaned by snow jet, and then by oxygen plasma during 10 minutes. The film under study is deposited by spin coating directly onto the quartz from a heptane solution. In the case of Sylgard 184, the film is crosslinked at $60\,^\circ$C during 24 hours. Then, the film-coated quartz is placed in a home-made cell and allowed to stabilize at $40\,^\circ$C during 1 hour.

We use an impedance analyzer (Solartron 1260A) to measure the admittance spectrum of the quartz resonator at different stages of the sample preparation. As shown in fig. 2(a), the resonance frequency f_0 is determined by curve fitting with a precision of $\Delta f_{min} = \pm 1$ Hz and the quality factor is obtained from $Q = f_0/\Delta f (\sim 10^5)$ where Δf is the width of the resonance peak. The deposition of the film lowers the resonance frequency of the crystal; the measurement of such a frequency shift allows determining the thickness of the film [11]. When mounting the quartz into the measurement cell, slight fluctuations of the resonance peak amplitude are observed from one experimental run to another. However, the downward shifts of the resonance frequency are very reproducible.

In order to study the viscoelastic properties of a spin-cast thin film beyond the QCM application, we cover the film-quartz system with two kinds of glass beads (fig. 1(a)): one is smooth with an rms roughness $\sigma \sim 10$ nm

and of diameter $2R \approx 650\,\mu$m (Duke Scientific) used for studying the cross-linked films; the other is rough with $\sigma \sim 100$ nm and of diameter $2R \approx 400\,\mu$m (Centraver) used for liquid films. Rough beads allow trapping the liquid film at the contact and limiting the squeeze flow. The roughness of the bead was measured with an AFM in contact mode. As shown fig. 2(a), covering the film with glass beads results in a totally different behavior than usual mass loading. We observe an increase of the resonance frequency Δf^+ after the deposition of beads, and a decrease of the resonance amplitude together with a peak broadening. These results clearly indicate elastic enhancement and dissipation increase of the quartz resonator.

Viscoelasticity of crosslinked films. – To gain physical insight into our resonance measurements, we model the quartz/film/smooth beads assembly as a pair of coupled oscillators (figs. 1(b), (c)). As in a previous work [14], the quartz resonator can be viewed as an effective masse M attached to a spring of shear stiffness K, determined from the fundamental resonance frequency $K = M\omega_0^2$. The glass bead of mass m is attached to the resonator M via the adsorbed film of thickness h. This film is modeled by a Kelvin-Voigt element involving a spring of shear stiffness k and a damping constant G'' (see fig. 1(c) and discussions below). No-slip boundary conditions are assumed here between both the film-bead and quartz-film interfaces, which are ensured by the strong adsorption of polymer films considered here.

Two eigenmodes exist for such coupled oscillators system with a natural frequency either superior (ω^+) or inferior (ω^-) to the quartz frequency ω_0. The ω^--mode corresponds to an *in-phase* motion between m and M giving access to the mass deposition by beads (not discussed here), while the ω^+-mode corresponds to an *out-of-phase* motion. The ω^+-mode is detected by the quartz crystal (fig. 2 (inset)) and to first-order approximation in k, the associated frequency shift $\Delta\omega^+(= \omega^+ - \omega_0)$ induced by the layer of beads reads:

$$\Delta\omega^+ \approx N_b k/2\sqrt{(MK)}, \qquad (1)$$

where $K = 3.6 \times 10^9$ N/m and $M = 3 \times 10^{-5}$ kg and N_b is the number of beads effectively covering the quartz electrode. The order of the minimum shear stiffness k_{min} that can be measured with this experiment is then a function of the beads number. Assuming that the oscillation of each bead is identical, the determination of $\Delta\omega^+$ enables us to characterize the elastic enhancement (stiffening) and properties of the adsorbed or bonded films. Indeed, if L is the lateral extent of the contact area (fig. 1(b)), we can estimate the elastic modulus of the film by $G'kh/(\pi L^2)$ where h corresponds to the sheared thickness at the contact zone.

Figure 2(b) shows clearly a linear dependence of Δf^+ as a function of N_b, obtained with a crosslinked Sylgard film of 265 nm and the smooth beads. The beads were placed on the spin-coated quartz by two different ways.
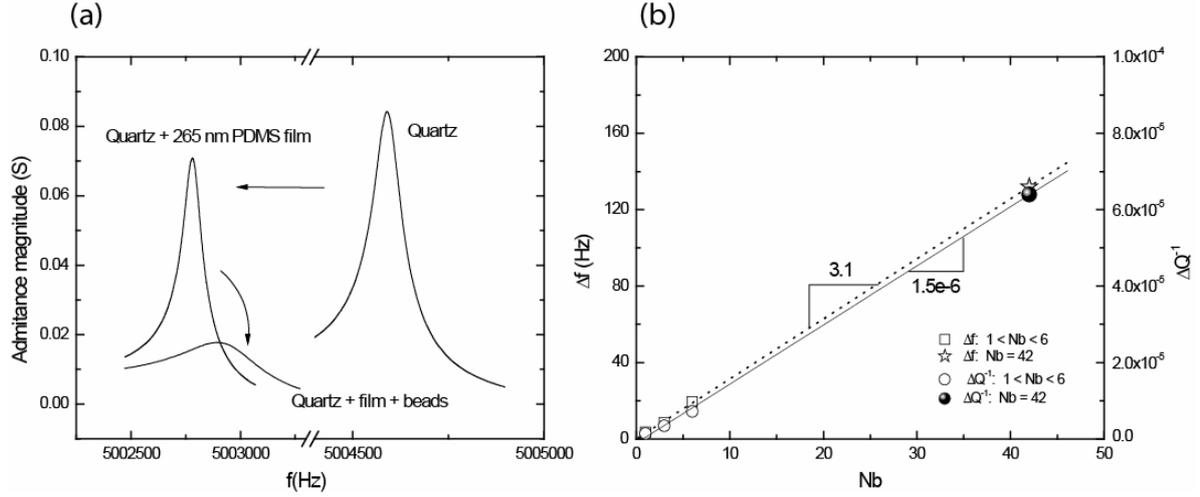
Fig. 2: (a) Negative frequency shift due to the mass deposition of a 265 nm crosslinked Sylgard film and positive frequency shift after deposition of the beads ($2R \approx 650\,\mu m$). (b) Evolution of resonance frequency and dissipation factor after deposition of a growing number of beads N_b. The value for $N_b \approx 40$ is evaluated using the effective surface area of the electrode (see text).

i) For a small number of beads $N_b = 1$, 3, 6, we used a perforated metallic disk mounted above the quartz. The disk was then approached by a microcontrol up to $\sim 50\,\mu m$ from the quartz and the beads were placed on the surface through the holes. ii) For a large number of N_b, a monolayer of beads was gently poured on the spin-coated quartz, resulting in a regular hexagonal packing such that $N_b \sim (2/3^{1/2}/4R^2)S \sim 40$, where S is the electrode surface area. Note that in the case of the monolayer, possible contacts between the beads do not alter the expected frequency shift.

In addition, the relative motion between the beads and the quartz resonator, inherent to the ω^+-mode, enhances strongly the shear strain in the adsorbed film and induces an interfacial dissipation which shall be detectable with the quartz resonator. It has been shown previously that the interfacial dissipation between two *dry* rough solid surfaces is governed by the interplay of a frictional loss and an interfacial viscoelastic one [4]. However, in the presence of a viscoelastic film as the case here, the viscous loss appears predominant over the other contributions to the energy dissipation. To characterize such a loss, we estimate the energy dissipated per cycle of oscillation by shearing a thin film between a sphere and a flat surface (fig. 1(b)) is $\Delta W_{film} \approx \pi(\omega^+\eta)(\pi L^2/h)U$, where L is the lateral extent of the contact, η is the film viscosity, $U(\sim 1\,nm)$ is the vibration amplitude of the quartz. In terms of the inverse of quality factor $\Delta Q^{-1} = (2\pi)^{-1}(\Delta W_{film}/W_q)$ where $W_q = (1/2)KU^2$ is the stored energy in the quartz, the additional dissipated energy is written as ($\omega^+ \approx \omega_0$),

$$\Delta Q^{-1} = N_b(\pi L^2/h)KG'', \qquad (2)$$

where $G'' = \omega^+\eta$. Measurements of such ΔQ^{-1} allow us to determine the dynamic viscosity of a thin polymer film. Figure 2(b) shows the experimental results of ΔQ^{-1} measured as a function of N_b. The linear dependence between ΔQ^{-1} and N_b confirms again the prediction by our model. Note that when the quantitative determination of G' and G'' are conditioned by the uncertainty on the measurement of K, L and N_b (see the section below), the loss angle defined as $\tan\delta = G''/G'$ may provide a very useful parameter for the material characterization. Combining eqs. (1) and (2) yields readily:

$$\tan\delta \approx \Delta Q^{-1}/2(\Delta f^+/f_0). \qquad (3)$$

Let us now examine the viscoelastic properties of the elastic film. From eqs. (1) and (2), we can respectively infer G' and G'' of the polymeric film if the radius of the contact area L is known. We measure the contact radius $L \sim 46 \pm 7\,\mu m$ in a separate experiment with an optical microscope, by imaging the contour of the circular contact area through the glass bead. To determine the size of the contact area, we have first calibrated the additional magnification of the spherical lens (bead), by imaging a known periodically structured silica wafer achieved by optical lithography. From the data of fig. 2(b) we obtain the stiffness and the dissipation of a single bead contact $\Delta f^+ \sim 3.1\,Hz\,(k \sim 3 \times 10^4\,N/m)$ and $\Delta Q^{-1} \sim 1.5 \times 10^{-6}$ and deduce consequently $G' \sim 1.7 \pm 0.5\,MPa$ and $G'' \sim 2.1 \pm 0.5\,MPa$. Such values are close to those obtained for bulk polydimethylsiloxane at same frequencies [15,16]. From eq. (3) we obtain $\tan\delta \sim 1.2$, again corresponding to bulk PDMS.

Further measurements performed with the rougher beads ($\sigma \sim 100\,nm$) of $2R \sim 200\,\mu m$ provide for one bead contact $\Delta f^+ \sim 0.6\,Hz\,(k = 7.2 \times 10^3\,N/m)$ and $\Delta Q^{-1} \sim 4.2 \times 10^{-7}$. With $L \sim 30 \pm 5\,\mu m$ as measured before we obtain $G' \sim 0.8 \pm 0.5\,MPa$, $G'' \sim 1.4 \pm 0.5\,MPa$ and $\tan\delta \sim 1.8$. The order of magnitude of these values
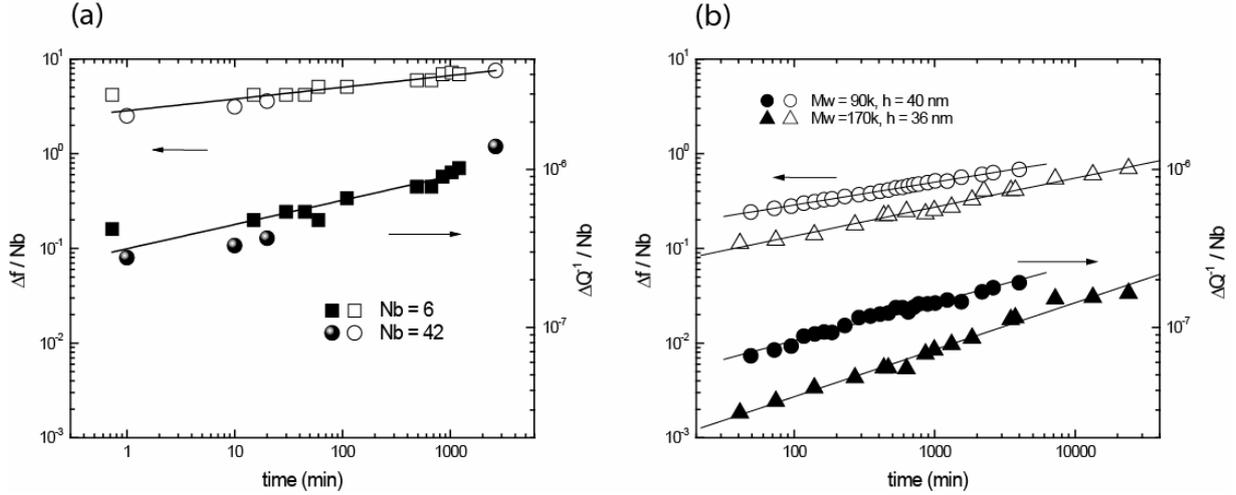
Fig. 3: Elasticity and dissipation as a function of time for crosslinked and liquid films of similar thicknesses. (a) 45 nm Sylgard film; plain lines represent a fit to a power law $\Delta f^+ \sim t^{0.12}$ and $\Delta Q^{-1} \sim t^{0.15}$. (b) 40 nm liquid films; the plain lines represent a fit to a power law $\Delta f^+ \sim t^{0.23}$ and $\Delta Q^{-1} \sim t^{0.23}$ for the 90k film, and $\Delta f^+ \sim t^{0.30}$ and $\Delta Q^{-1} \sim t^{0.28}$ for the 170k film.

is in agreement with the above results. The concordance with bulk properties was expected due to the very local probe provided by the present method. At such high frequency, only Rouse modes are relevant (size $<$ nm) and no confinement effect may arise until the thickness of the film reaches the characteristic size of those modes. The above results confirm thus the validity of the present method for characterizing the viscoelastic properties of elastic films.

Aging and wetting phenomena. – Figure 3(a) shows $\Delta f^+/N_b$ and $\Delta Q^{-1}/N_b$ for a 45 nm Sylgard film crosslinked in the same conditions, using the smooth beads. Unlike the response for the 265 nm film which was stable, the frequency shift and the dissipation factor evolve in time like $\Delta f^+ \sim \Delta Q^{-1} \sim t^{0.12-0.15}$. This ageing effect is not related to an ultrasonic excitation. Indeed, as shown fig. 3(a), the acoustic responses acquired at different time intervals of ultrasonic measurements are similar. However, the mechanism of this ageing or creep is still unclear. The crosslinking of the Sylgard 184 could be different from the bulk and the thin film might be poorly cured, thus exhibiting a liquid-like behavior. In such a case L and h could vary with time, causing in turn the evolution of Δf^+ and ΔQ^{-1}. Instead of determining the dynamic moduli from eqs. (1) and (2) which requires the time dependence of L and h not available in the present study, we seek to estimate the loss angle of the film, $\tan \delta$, from eq. (3) since Δf^+ and ΔQ^{-1} undergo a similar temporal evolution. Figure 4(a) provides an effective $\tan \delta \sim 0.5$, slightly lower than that for a thicker film.

To further study the aging effect, we investigate as well liquid —uncrosslinked— PDMS films of mass $M_w \sim 90000$ of thicknesses between 9 and 80 nm. The rough beads of

$2R \sim 400\,\mu$m and $\sigma \sim 100$ nm were used to minimize the squeezing effect. Some results are illustrated in fig. 3(b), which show the ageing behavior for both Δf^+ and ΔQ^{-1}, roughly varying as $\sim t^{0.30 \pm 0.05}$. Here the error is calculated from the standard deviation of four similar experiments and is also representative of the data dispersion on the other power law exponents discussed in this work. This could be related to the wetting on the free surface of the glass beads by the polydimethylsiloxane thin film as indicated by eqs. (1) and (2). Indeed, taking into account the surface energies of the PDMS and glass, we may expect a total wetting process, following a power law $L \sim (\gamma t/\eta)^{\alpha}$ where γ is the surface tension of the PDMS and α is an exponent characteristic of the details of the wetting process [17]. This scenario is supported in part by the observation of the contact radius evolution $L \sim t^{0.16 \pm 0.04}$ with optical microscopy. Further evidence arises from fig. 3(b) where we show the ageing of a polymer of $M_w \sim 170000$ with a higher viscosity such that $\eta \sim M_w^{3.4}$ [18], corresponding qualitatively to the wetting law given above. The detailed study of these wetting-related issues is however beyond the scope of this work and will be treated in the future.

Before examining the viscoelastic properties of the liquid films from Δf^+ and ΔQ^{-1}, we discuss some other mechanisms which may be responsible for the stiffness enhancement. In the case of liquid films, the beads make direct contacts with the quartz surface which could induce additional elastic enhancement and dissipation from solid-solid contact. As shown in fig. 4(b), a characteristic frequency shift for a 40 nm liquid film is about $\Delta f^+/N_b \sim$ 0.1–1 Hz which corresponds to a stiffness of the order of $k \sim 10^3$–10^4 N/m for one bead contact. Dybwad [19] previously reported such a stiffness magnitude between
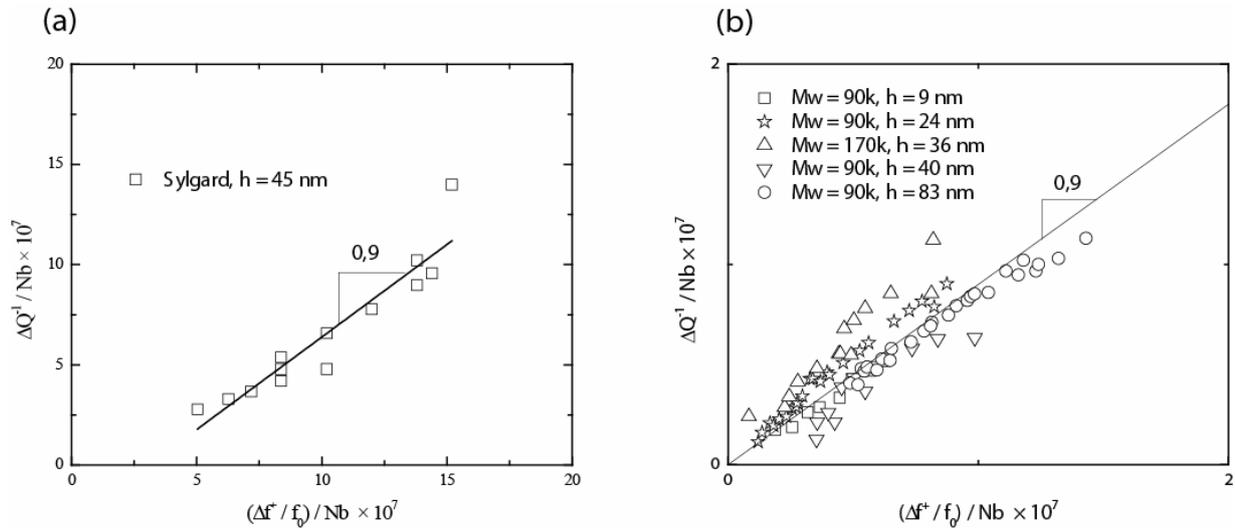
Fig. 4: Measured ΔQ^{-1} plotted *vs.* $\Delta f^+/f_0$. (a) Crosslinked elastomer. (b) Liquid PDMS. The plain lines show linear scaling as predicted by eq. (3).

a smooth Au sphere and an Au-coated quartz resonator, originating from van der Waals bonds. This cohesion is not observed in our resonance measurements when the glass beads are deposited on the *bare* quartz crystal. This may be related to the roughness of the beads, which provides a contact stiffness for the multicontact interface, $k_{MCI} = N/\lambda \sim 1\,\mathrm{N/m}$, with N the normal load and λ the elastic length of the order of microns [20]. Such a value is too low to be detected with our present apparatus. On the other hand, the presence of wetting films creates a capillary interaction F_c between the beads and the resonator which could stiffen the above contact stiffness. However, an estimation of the capillary force on a wet rough surface yields at *maximum* a capillary force about $F_c = 2\pi\gamma R, \ \sim 10^{-5}\,\mathrm{N}$ [21], as in the case between smooth spheres. However, the increase of the normal loading N by this capillary force F_c would give rise to a *shear* contact stiffness of $k \sim 10\,\mathrm{N/m}$, much less than the elastic enhancement observed in our experiments. This implies that the capillary effect should not affect the shear contact stiffness studied in our work, yet it can contribute to the normal stiffness [22].

Note that only a part of the thin film located under the bead is in true contact with the bead. However, the elastic modulus G' of the order of $1\,\mathrm{MPa}$ corresponds to a wave speed of about $30\,\mathrm{m/s}$. At the frequency of the resonator ($5\,\mathrm{MHz}$), the wavelength is then $\lambda \approx 6\,\mu\mathrm{m}$, which is larger than the distance between asperities ($\sim 1\,\mu\mathrm{m}$). Therefore, all film located at the contact area within L is sheared almost uniformly via the asperities, contributing to the stiffness enhancement and the dissipation observed. Again, evaluating G' and G'', respectively, from eqs. (1) and (2) requires the details of the wetting dynamics $L(t)$ from a thin film onto a rough surface, which is not available at this stage. However, the similar time dependencies of Δf^+ and

ΔQ^{-1} suggests the use of eq. (3), providing $\tan\delta \sim 0.4$–0.7 (see fig. 4(b)). This is close to the Sylgard elastomer of same thickness.

Conclusion. – In summary, we have developed an ultrasonic method for measuring the high-frequency viscoelastic properties of thin polymeric films. For the crosslinked films of about $250\,\mathrm{nm}$, both shear modulus G' and viscous dissipation G'' are determined. Our results indicate that the viscoelastic properties of such polymer films are not quantitatively different from those of the bulk. For liquid films and thinner crosslinked films ($h < 100\,\mathrm{nm}$), wetting and ageing behavior render difficult the direct determination of G' and G'' at this stage. However, one can adequately estimate the loss angle $\tan\delta$ of the films when the elastic stiffening and dissipation arise from the same geometric structure. An effective loss angle is obtained which is lower than that for the thick crosslinked films. Further work is needed to perform time-resolved measurements of thickness and contact area in order to better appreciate the variation of $\tan\delta$ with film thickness.

We believe that by using beads of different surface properties and controlling ambient conditions, this ultrasonic method provides a promising tool for exploiting the confinement effects of nanometric films, the interfacial dynamics and the wetting phenomena at various boundaries [2,23].

$* * *$

REFERENCES

[1] Urbakh M., Klafter J., Gourdon D. and Israelachvili J. N., *Nature*, **430** (2004) 525.
[2] He G., Muser M. H. and Robbins M. O., *Science*, **284** (1999) 1650.
[3] Bocquet L., Charlaix E., Ciliberto S. and Crassous J., *Nature*, **396** (1998) 735.
[4] Brunet Th., Jia X. and Mills P., *Phys. Rev. Lett.*, **101** (2008) 138001.
[5] Stafford C. M., Harrison C., Beers K. L., Karim A., Amis E. J., VanLandingham M. R., Kim H. C., Volksen W., Miller R. D. and Simonyi E. E., *Nat. Mater.*, **3** (2004) 545.
[6] Bodiguel H. and Frétigny C., *Phys. Rev. Lett.*, **97** (2006) 266105.
[7] Bureau L. *et al.*, *Rev. Sci. Instrum.*, **78** (2007) 065110.
[8] Wu H. W., Carson G. A. and Granick S., *Phys. Rev. Lett.*, **66** (1991) 2758.
[9] Gee M. G., McGuiggan P. M., Israelachvili J. N. and Homola A. M., *J. Chem. Phys.*, **93** (1991) 1895.
[10] Sun G., Kappl M. and Butt H. J., *Colloids Surf. A*, **250** (2004) 203.
[11] Ballantine D. S., White R. M., Martin S. J., Ricco A. J., Zellers E. T., Frye G. C. and Wohltjen H., *Acoustic Wave Sensors* (Academic Press, San Diego) 1997.
[12] Royer D. and Dieulesaint E., *Elastic Waves in Solids,* Vol. **2**: *Generation, Acousto-optic Interaction, Application* (Masson, Paris) 1999, in French.
[13] Ogi H., Fujii M., Nakamura N., Yatsui T. and Hirao M., *Phys. Rev. Lett.*, **98** (2007) 195503.
[14] Wolff O. and Johannsmann D., *J. Appl. Phys.*, **873** (2000) 4182.
[15] Rahalker R. R., Lamb J., Harrison G., Barlow A. J., Hawthorn W., Semlyen J. A., North A. M. and Pethrick R. A., *Proc. R. Soc. London, Ser. A*, **394** (1984) 207.
[16] Longin P. Y., Verdier C. and Piau M., *J. Non-Newt. Fluid Mech.*, **76** (1998) 213.
[17] De Gennes P. G., *Rev. Mod. Phys.*, **57** (1985) 827.
[18] De Gennes P. G., *Scaling Concepts in Polymer Physics* (Cornell University Press, Ithaca, NY) 1979.
[19] Dybwad G. B., *J. Appl. Phys.*, **58** (1985) 2789; D'Amour J. N., Stålgren J. J. R., Kanazawa K. K., Frank C. W., Rodahl M. and Johannsmann D., *Phys. Rev. Lett.*, **96** (2006) 058301.
[20] Berthoud P. and Baumberger T., *Proc. R. Soc. London, Ser. A*, **454** (1998) 1615.
[21] Halsey T. C. and Levine A. J., *Phys. Rev. Lett.*, **80** (1998) 3141.
[22] Crassous J., Charlaix E. and Loubet J. L., *Phys. Rev. Lett.*, **78** (1997) 2425.
[23] Krim J., Solina D. H. and Chiarello R., *Phys. Rev. Lett.*, **66** (1991) 181.